

Real-Time Estimation of the Ventricular Relaxation Time Constant

Honggu Chun, Hee Chan Kim, Daewon Sohn¹

Department of Biomedical Engineering, College of Medicine &
Institute of Biological & Medical Engineering, Medical Research Center
¹Department of Internal Medicine, College of Medicine, Seoul National University
(Received September 22, 2004. Accepted February 17, 2005)

Abstract: A new method for real-time estimating left ventricular relaxation time constant (τ) from the left ventricular (LV) pressure waveform, based on the isovolumic relaxation model, is proposed. The presented method uses a recursive least squares (RLS) algorithm to accomplish real-time estimation. A new criterion to detect the end-point of the isovolumic relaxation period (IRP) for the estimation of τ is also introduced, which is based on the pattern analysis of mean square errors between the original and reconstructed pressure waveforms. We have verified the performance of the new method in over 4,600 beats obtained from 70 patients. The results demonstrate that the proposed method provides more stable and reliable estimation of τ than the conventional 'off-line' methods.

Key words: Ventricular relaxation time constant, Ventricular diastolic function, Real-time estimation, Recursive least squares algorithm

INTRODUCTION

Over several decades, the analysis of LV diastolic function has received continued attention, because LV diastolic dysfunction is recognized as an important primary cause of heart failure [1, 2]. Among the many parameters that attempt to describe diastolic function, τ has been widely applied in both experimental and clinical studies [3-6].

Weiss et al proposed that the LV pressure during the IRP can be modeled as a simple exponential function of time [5]. IRP is defined to be from the time of semilunar valve closing to mitral valve opening as shown in Fig. 1. They quantified the LV relaxation rate by fitting the time course of the isovolumic pressure fall beginning at the time of the $dP(t)/dt$ negative peak and ending with mitral valve opening with the exponential function.

where P_0 , t , τ are the pressure at $dP(t)/dt$ negative peak, the time lapsed after the $dP(t)/dt$ negative peak and time constant of isovolumic LV pressure fall, respectively. A convenient way to compute τ in eq. (1) is to take the natural logarithm of both sides of equation. It yields a linear relation between $\ln P(t)$ and t , with a slope of $-1/\tau$. Then τ can be estimated by linear regression.

Eq. (1) was modified to take into account the effect of unequal end-systolic and equilibrium volumes by incorporating the term, P_∞ , which is the pressure that the ventricle would relax to if it were held at its end-systolic volume and allowed to relax completely [7].

$$P(t) = P_0 e^{-\frac{t}{\tau}} \quad (1)$$

$$P(t) = (P_0 - P_\infty) e^{-\frac{t}{\tau}} + P_\infty \quad (2)$$

Although incorporation of P_∞ in eq. (2) improves the accuracy with which it describes relaxation, the presence of P_∞ complicates the calculation of τ because the natural logarithm of both sides of eq. (2) no longer yields a linear relation between pressure and time.

Other methods for determination of τ have also been proposed, including polynomial fitting, two-sequential

This work was supported in part by the Advanced Biometric Research Center (ABRC) through the Korea Science and Engineering Foundation.

Corresponding Author: Hee Chan Kim, Ph.D. Department of Biomedical Engineering Seoul National University Hospital 28 Yongon Dong, Chongno Gu, Seoul, 110-744, KOREA
Tel. 822-2072-2931, Fax. 822-747-8597
E-mail. hckim@snu.ac.kr

monoexponential model, pressure half time, best exponential curve fit and logistic time constant method. [6,8-11]. Paulus et al. showed that calculations based on Weiss model yielded a time constant that was close to the value derived with the measured diastolic LV asymptote pressure of the nonfilling beat [4]. Thus, from a practical point of view, among the models described above, Weiss model is generally accepted as a reasonable clinical measure of how quickly the ventricle relaxes [1, 2]. We followed the Weiss model during this study.

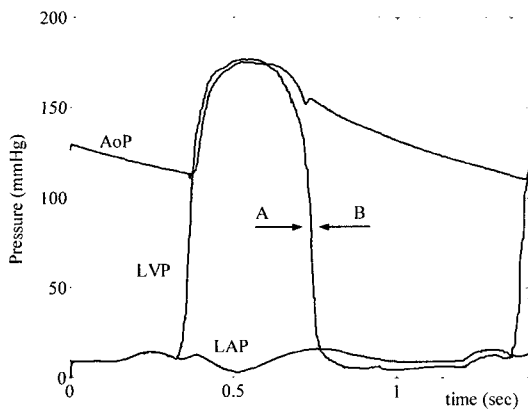


Fig.1. Definition of IRP. IRP is defined from semilunar valve closing (arrow A) to mitral valve opening (arrow B). LVP (Left Ventricular Pressure), LAP (Left Atrium Pressure), AoP (Aortic Pressure)

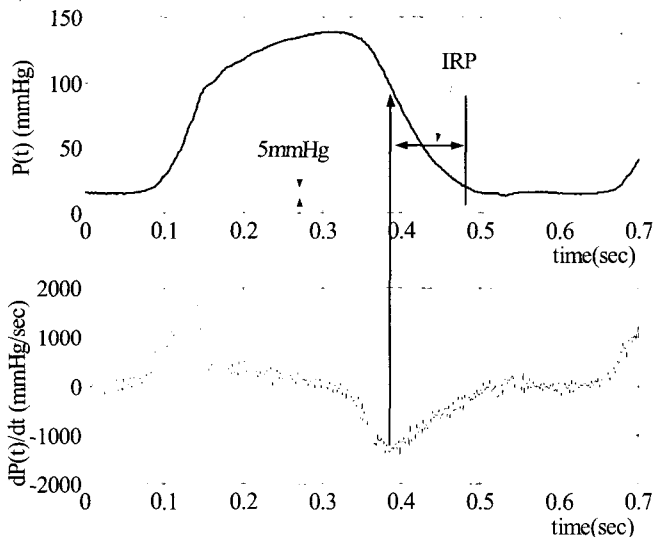


Fig.2. Conventional criterion to define IRP. IRP begins at negative peak of $dP(t)/dt$ and ends at the point 5 mmHg above the end diastolic LV pressure, $P(t)$, of the previous beat.

In conventional studies, the start-point of IRP is chosen when the derivative of pressure waveform shows a negative peak [Fig. 2]. Since the negative peak equates to the steepest decaying point, it must occur within the early phase of IRP, we adopted this criterion in our study. However, to define the end-point of IRP, one needs to measure LV and left atrial pressure simultaneously [11]. But, in clinical situation, it's difficult to measure left atrial pressure. Therefore, various criteria to define the end-point of IRP were proposed. For example, the end-point of IRP is defined as the point at which the LV pressure had decayed to the same level of the end diastolic pressure of previous beat, a value of 5 mmHg above the end diastolic pressure of the previous beat (as shown in Fig. 2) and a value of 10 mmHg above the end diastolic pressure of the previous beat [11]. But, none of them has achieved general acceptability. The calculated τ value is very dependent upon the position of the IRP end-point [Fig. 3(a)], and it might be considered to be somewhat arbitrary to define the end-point in this manner. Also, in certain patients who have, for example, premature beat or tachycardia, it may not be possible to locate the end-point as defined by the criterion described above [Fig. 3(b)]. Thus, we believed that there was a need to define an objective and practically useful definition for the IRP end-point.

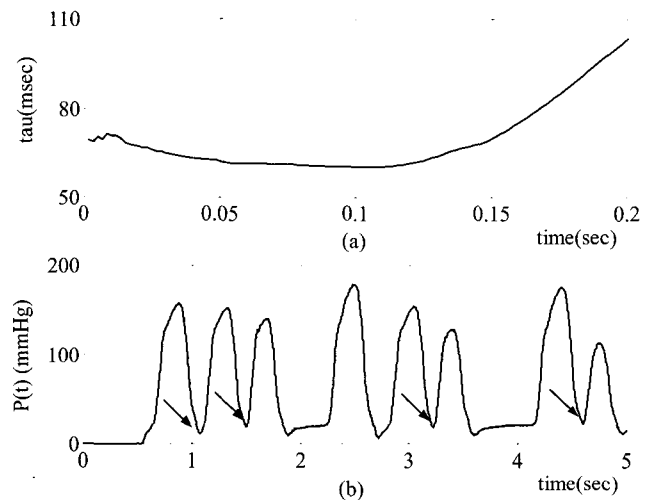


Fig.3. (a) Typical changes of τ as the end-point of the IRP moves incrementally from the IRP start-point. τ varies widely according to the location of the IRP end-point. (b) LV pressure waveform of atrial fibrillation patient. The four arrows indicate beats missed in detecting the end-point of IRP using conventional method.

Another difficulty in using τ arises from the fact that there exists no real-time calculation method. Every researcher, therefore, performs off-line calculations using recorded LV pressure waveforms. But, in some

clinical situation, it's critical to evaluate the hemodynamic conditions in real-time to avoid excessive treatment or experimental conditions that might permanently alter the physiologic condition [12].

In this paper, we propose, as a solution to both of the afore-mentioned problems, an objective criterion to find the IRP end-point based on a pattern analysis of mean square error profile, and a new real-time calculation method which derived a recursive representation of τ and mean square error. And we developed a software system that displays mean square error profile and an IRP end-point marker with LV pressure waveform to validate the criterion visually.

MATERIALS & METHODS

Overall Algorithm Description

The IRP start-point was chosen as the point at which the rate of decrease of pressure showed a negative peak in a beat. If the pressure waveform after the IRP start-point is expressed as a logarithm, this signal can be represented as a linear function of time, as is mentioned in Weiss model. At every new consecutive data sample point after the starting point, τ was calculated by linear regression. And the signal was reconstructed from the linear model using the measured P_0 and the calculated value of τ . And the mean square error between the logarithms of the original and reconstructed signals for all data points used in the estimation of τ was calculated. These calculation of τ and mean square error were iterated with the data sampling rate until the IRP end-point is detected by the criterion described below. τ is estimated based on the detected IRP end-point, and the algorithm is repeated with next beat.

Determination of IRP End-point

Typical pattern of τ and mean square error is shown in Fig. 4. Except initial few msec after the start-point of IRP where τ increases rapidly, τ starts with a decreasing pattern. Mean square error in this period is negligible. After τ shows a minimum value, it starts to increase. Then mean square error also increases rapidly. Mean square error in this period can be fitted as a linear function of time and the end-point of the IRP is chosen as a point where this linear function crosses the time axis. The period for the linear fitting of mean square error is chosen where mean square error exceeds 0.01mmHg^2 continuously for 10% of beat period. These threshold values were chosen by analyzing about 4,600 cycles of the LV pressure waveform collected from 70 patients so that the estimation is robust to noise. The rapid increase of

error means that the data sample concerned was taken after the end-point of the IRP. Thus, it is reasonable to take this point as the end-point of IRP and to determine τ based on this point. The reason why τ increases at this point is that filling of the LV, caused by mitral valve opening, inhibits the continuing rapid exponential pressure decay. The arrows in Fig. 4 indicate the end-point of IRP chosen by this criterion.

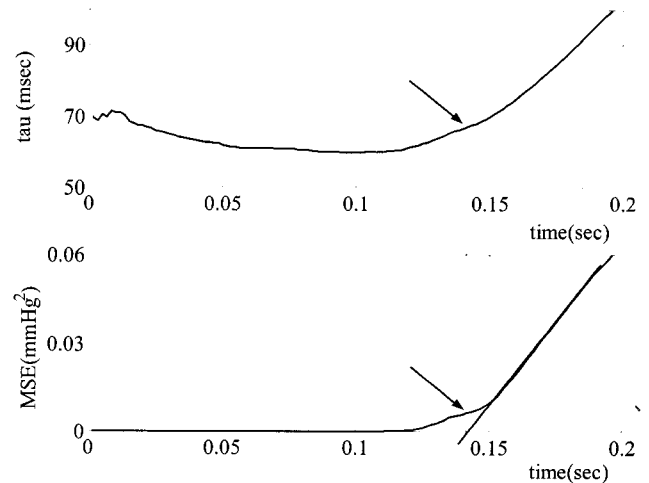


Fig.4. Typical pattern of τ and mean square error (MSE). After τ shows a minimum value, mean square error increases rapidly. Mean square error in this period can be fitted as a linear function of time and the end-point of the IRP is chosen as a point where this linear function crosses the time axis. The arrow indicates the end-point of IRP chosen by this criterion.

Calculation of τ and Mean Square Error

Estimating τ and calculating the mean square error is performed by; 1) finding the IRP start-point, and 2) calculating τ and the mean square error, iteratively, to find the IRP end-point.

Firstly, the start-point detection procedure is as follows;

- 1) Real-time data is filtered by a causal FIR differentiator windowed with an 11th order rectangular window,

$$h_{diff}(i) = \frac{\cos \pi(i-5)}{i-5} - \frac{\sin \pi(i-5)}{\pi(i-5)^2}, \quad 0 \leq i \leq 10 \quad (3)$$

- 2) Noise that is amplified during differentiation is suppressed by a causal FIR lowpass filter windowed

with an 11th order rectangular window, of cutoff frequency $\frac{\pi}{6}$,

$$h_{low}(i) = \frac{\sin \frac{\pi}{6}(i-5)}{i-5}, \quad 0 \leq i \leq 10 \quad (4)$$

3) Then, the output can be expressed as:

$$p_{diff}(i) = p(i) * h_{diff}(i) * h_{low}(i) \quad (5)$$

where, $p(i)$ is the sampled LV pressure data.

4) The IRP start-point is obtained by finding negative peak of $p_{diff}(i)$ [Fig. 2].

Secondly, τ and the mean square error calculation and the determination of the IRP end-point are performed as follows;

In order to get a linear model, eq. (1) is converted into its natural logarithmic form and the equation represented as a discrete matrix,

$$\ln p(i) = -\frac{1}{\tau}t_i + \ln p(0) = \underline{t}_i^T \underline{w},$$

$$\text{where } \underline{t}_i = \begin{bmatrix} t_i \\ 1 \end{bmatrix} \text{ and } \underline{w} = \begin{bmatrix} -\frac{1}{\tau} \\ \ln p(0) \end{bmatrix}, \quad (6)$$

where t_i denotes the i -th sampling time after the start-point of IRP at $t_0 = 0$.

We define a vector, $\underline{q}(m)$, as the accumulated vector of measured pressure in logarithmic form, $\ln p_m(i)$, and the accumulated time matrix, T_m , up to the m -th data point as follows,

$$\underline{q}(m) = \begin{bmatrix} \ln p_m(m) \\ \ln p_m(m-1) \\ \vdots \\ \ln p_m(2) \\ \ln p_m(1) \end{bmatrix}, \quad T_m = \begin{bmatrix} t_m & t_{m-1} & \cdots & t_2 & t_1 \end{bmatrix}^T \quad (7)$$

Then, the total square error between measured and the reconstructed pressure waveforms for m data samples is given by,

$$e(m) = (\underline{q}(m) - T_m \underline{w})^T (\underline{q}(m) - T_m \underline{w}) \quad (8)$$

The least square error method provides the optimum weight vector using the following equation,

$$\hat{\underline{w}}_m = (T_m^T T_m)^{-1} T_m^T \underline{q}(m) \quad (9)$$

5) By definition, the estimated τ for m data samples in the IRP, $\hat{\tau}$, is obtained from the first element of $\hat{\underline{w}}_m$.

6) From eq. (8), calculate the mean square error, $\frac{\hat{e}_m}{m}$, between the logarithm of the measured and calculated pressure waveforms.

7) Determine whether the end-point of the IRP is reached or not by interpreting the mean square error pattern using the criteria proposed previously.

8) Repeat from 5) to 7) with the next $(m+1)$ th data sample until the IRP reaches end-point.

The iterative calculations for τ and mean square error results in increased number of operations. In order to achieve real-time operation, each iteration should be performed within one sampling period of 1/600 second. If the given data number is m , conventional method[4] requires $6m+10$ multiplications and $6m-3$ additions to calculate $\hat{\underline{w}}_m$, i.e. $O(m)$. The proposed algorithm needs $5.5m^2+15.5m$ multiplications and $5.5m^2+1.5m$ additions to calculate $\hat{\underline{w}}_m$ and $\hat{e}(m)$, i.e. $O(m^2)$. As the number of data points increases, the computational load increases rapidly. In the case of 600 Hz sampling, the average length of the IRP is 100 samples and the proposed method requires 92 more operations than conventional calculation. It was, therefore, necessary to develop a recursive algorithm for the real-time estimation of $\hat{\underline{w}}_m$ and $\hat{e}(m)$.

Recursive Algorithm for the Real-Time Estimation of τ and Mean Square Error

To develop the recursive formula of eq. (8) and (9), a RLS algorithm based upon a linear regression model can be used [13]. The application of such an RLS algorithm yields the following set of equations for τ and the mean square error:

$$\hat{\mathbf{w}}_m = \hat{\mathbf{w}}_{m-1} + \underline{\mathbf{k}}_m \xi_m \quad (10)$$

$$\hat{e}_m = \hat{e}_{m-1} + \zeta_m \xi_m \quad (11)$$

where ξ_m and ζ_m are the *a priori* and *a posteriori* estimation errors defined by

$$\xi_m = \hat{q}_m - \underline{\mathbf{t}}_m^T \hat{\mathbf{w}}_{m-1} \quad (12)$$

and

$$\zeta_m = \hat{q}_m - \underline{\mathbf{t}}_m^T \hat{\mathbf{w}}_m \quad (13)$$

, respectively.

And, a 2-by-1 gain vector $\underline{\mathbf{k}}_m$ which is defined by

$$\underline{\mathbf{k}}_m = \frac{\Phi_{m-1}^{-1} \underline{\mathbf{t}}_m}{1 + \underline{\mathbf{t}}_m^T \Phi_{m-1}^{-1} \underline{\mathbf{t}}_m} \quad (14)$$

where,

$$\Phi_m = T_m^T T_m = \sum_{k=1}^m \underline{\mathbf{t}}_k \underline{\mathbf{t}}_k^T = \sum_{k=1}^{m-1} \underline{\mathbf{t}}_k \underline{\mathbf{t}}_k^T + \underline{\mathbf{t}}_m \underline{\mathbf{t}}_m^T = \Phi_{m-1} + \underline{\mathbf{t}}_m \underline{\mathbf{t}}_m^T \quad (15)$$

By definition, the correlation matrix Φ_m is positive definite and therefore, nonsingular. Thus we may use matrix inversion lemma to obtain a recursive form of Φ_m^{-1} from eq. (15) [13]:

$$\Phi_m^{-1} = \Phi_{m-1}^{-1} - \frac{\Phi_{m-1}^{-1} \underline{\mathbf{t}}_m \underline{\mathbf{t}}_m^T \Phi_{m-1}^{-1}}{1 + \underline{\mathbf{t}}_m^T \Phi_{m-1}^{-1} \underline{\mathbf{t}}_m} \quad (16)$$

Thus, we can estimate both τ and the mean square error recursively from eq. (10)- (16).

The RLS method developed from equations (10) to (16) requires 26m multiplications and 19m additions, which is of the same order, $O(m)$, as conventional method.

RESULTS

About 4,600 cycles of the LV pressure waveform were collected from 70 patients who were undergoing cardiac catheterization procedure in Seoul National University Hospital. Left heart catheterization was performed by the femoral approach. A pacing electrode was placed in the high right atrium with pacing frequency of 100 beats/min. A 3F Millar transducer (Millar instruments, USA) was located within an 8F pigtail catheter or a 7F Millar transducer with a single lumen being introduced into the left ventricle. Digital pressure data was acquired using a commercial A/D converter EZAD512 (ELBIO, Korea) with a 12 bits resolution and a sampling rate of 600 Hz. An IBM compatible PC with Windows 2000 was utilized for data acquisition, real-time signal processing and data display. The software was written in Labview 6.0 (National Instruments, USA). Fig. 5 shows a window display of the developed software estimating τ in real-time. The chart in lower part displays LV pressure waveform acquired during catheterization procedure. The first chart in upper part shows the trajectory of τ of each beat estimated in real-time with the numeric value of τ at the current beat. Time-variation of τ and mean square error profile calculated iteratively for each beat are shown in the rest two charts. An IRP end-point marker is placed in mean square error profile chart to validate the criterion visually. One can calibrate LV pressure value at two points of 0 mmHg and 100 mmHg using two corresponding calibration buttons. LV pressure waveform and estimated τ values can be stored and loaded with appropriate file names for further study.

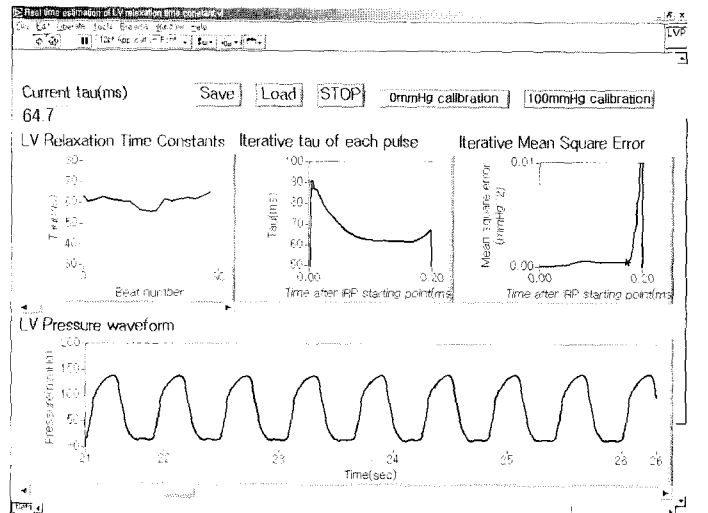


Fig.5. Window display of the developed software estimating τ in real-time. It displays LV pressure waveform and the trajectory of τ of each beat in real-time. An IRP end-point marker is placed in mean square error profile chart to validate the criterion visually.

Table 1. An example that shows the robustness of proposed method. This shows τ values (in msec) of each beat estimated from conventional and proposed method for LV pressure waveform shown in Fig. 3(b).

Beat Sequence		1	2	3	4	5	6	7	8
Estimated tau [msec]	Conventional method	N/A	N/A	56.3	45.3	N/A	61.8	N/A	65.0
	Proposed method	55.5	65.6	59.5	61.6	56.1	58.7	73.2	70.5

Fig. 6 shows a 2-D scatter plot of LV pressure at the IRP end-point obtained by conventional and proposed criterion for 70 patients. Each method yields a distribution of 14.8 ± 5.82 mmHg and 13.6 ± 8.78 mmHg (mean \pm SD), respectively, which implies that the conventional method locates the end-point of IRP in more conservative manner so that it generated a narrower range of the pressure value at the end-point of IRP. Since the dependence of τ on IRP end-point is significant, it can be postulated that conventional criterion with a constant offset pressure is incomplete and proposed criterion with the pattern analysis of mean square error of each beat is more reliable.

LV pressure waveform in Fig. 3(b) is an example where the conventional method fails to produce stable results. Table 1 shows τ values of each beat estimated from conventional and proposed method. As it shows, τ can be calculated without a missing beat in such an unstable condition using the proposed method. As is shown by the results, our method yields more robust and reliable estimation of τ .

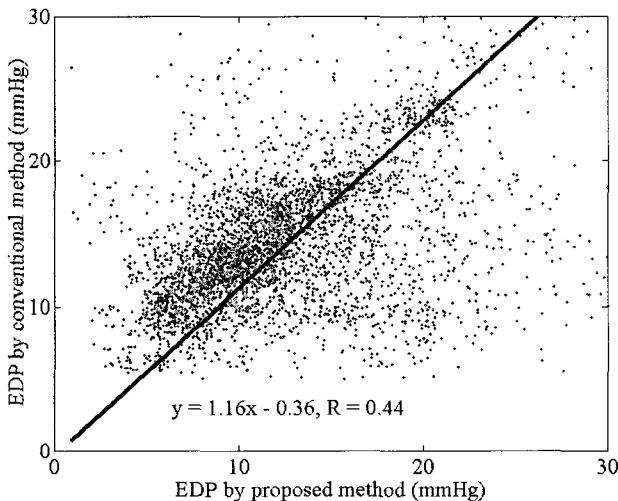


Fig.6. A 2-D scatter plot of LV pressure at the IRP end-point obtained by conventional (y-axis) and proposed criterion (x-axis) for 70 patients. Each method yields a distribution of 14.8 ± 5.82 mmHg and 13.6 ± 8.78 mmHg (mean \pm SD), respectively. Regression result is $y = 1.16x - 0.36$ and correlation coefficient $R = 0.44$.

CONCLUSIONS

In conclusion, a new method and a program to detect the IRP end-point for real-time τ estimation is proposed. The method is based on pattern analysis of the mean square error profile, and its performance is shown to be more reliable than the conventionally used methods. The total number of calculations can be maintained to the same order as the conventional method by incorporating the RLS method which also enables the real-time estimation of τ .

This algorithm was implemented on a PC based system so that it is possible to estimate τ in real-time from LV pressure waveform acquired during cardiac catheterization procedure. It will be a useful tool in clinical situations, for example, evaluating the state of ischemia to avoid permanent damage of the heart. The usage of proposed algorithm can be extended to any linear or monoexponential model that needs real time estimation.

REFERENCES

- [1] A.H. Dougherty, G.V. Naccarelli, E.L. Gray, C.H. Hicks, and R.A. Goldstein, "Congestive heart failure with normal systolic function", *Am J Cardiol.*, Vol. 54, pp.778-782, 1984.
- [2] K.M. Kessler, "Heart failure with normal systolic function-update of prevalence, differential diagnosis, prognosis and therapy", *Arch Intern Med.*, Vol. 148, pp.2109-2111, 1988.
- [3] D.W. Sohn, I.H. Chai, D.J. Lee, H.C. Kim, H.S. Kim, B.H. Oh, M.M. Lee, Y.B. Park, Y.S. Choi, J.D. Seo, and Y.W. Lee, "Assessment of Mitral Annulus Velocity by Doppler Tissue Imaging in the Evaluation of Left Ventricular Diastolic Function", *J Am Coll Cardiol.*, Vol. 30, pp.474-480, 1997.
- [4] W.J. Paulus, P.J. Vantrimpont, and M.F. Rousseau, "Diastolic Function of the Nonfilling Human Left Ventricle", *J Am Coll Cardiol.*, Vol. 20, pp.1524-1532, 1992.
- [5] J.L. Weiss, J.W. Frederiksen, and M.L. Weisfeldt, "Hemodynamic determinants of the time-course of fall in canine left ventricular pressure", *J Clin Invest.*, Vol. 58, pp.751-760, 1976.
- [6] I. Mirsky, "Assessment of diastolic function: Suggested methods and future consideration", *Circulation*, Vol. 69, pp.836-841, 1984.
- [7] J.C. Gilbert, S.A. Glantz, "Determinants of Left Ventricular Filling and of the Diastolic Pressure-Volume Relation", *Circ Res.*, Vol. 64, No.5, pp.827-852, 1989.
- [8] G.L. Raff, S.A. Glantz, "Volume loading slows left

- ventricular isovolumic relaxation rate: Evidence of load-dependent relaxation in the intact dog heart*", *Circ Res.*, Vol. 48 (June), pp.813-824, 1981.
- [9] D.S. Thompson, C.B. Waldron, D.J. Coltart, B.S. Jenkins, and M.M. Webb-Peploe, "Estimation of time constant of left ventricular relaxation", *Br Hear J.*, Vol. 49, pp.1426-1434, 1985.
- [10] W.J. Paulus, B.H. Lorell, W.E. Craig, J. Wynne, J.P. Murgu, and W. Grossman, "Comparison of the effects of nitroprusside and nifedipine on diastolic properties in patients with hypertrophic cardiomyopathy: Altered left ventricular loading or improved muscle inactivation.?", *J Am Coll Cardio.*, Vol. 2, pp.879-886, 1983.
- [11] H. Matsubara, M. Takaki, S. Yasuhara, J. Araki, H. Suga, "Logistic time constant of isovolumic relaxation pressure-time curve in the canine left ventricle", *Circulation*, Vol. 92, pp.2318-2326, 1995.
- [12] W. Hu, B. Leone, "A graphic orientated data analysis system for hemodynamic research", *Comput. Prog. Biomed.*, Vol. 59, pp.197-214, 1999.
- [13] S. Haykin, *Adaptive filter theory*, 3rd edition, pp.562-587, USA: Prentice-Hall, 1996.